Impedance Spectroscopy on Polymer-Fullerene Solar Cells

Martin Knipper[a], Jürgen Parisi[a], Kevin Coakley[b], Christoph Waldauf[b], Christoph J. Brabec[b], and Vladimir Dyakonov[c]

[a] Energy and Semiconductor Research Laboratory, Department of Physics, University of Oldenburg, D-26111 Oldenburg, Germany
[b] Konarka Technologies Germany, Landgrabenstraße 94, D-90443 Nürnberg, Germany
[c] Faculty of Physics and Astronomy, University of Würzburg, Am Hubland, D-97074 Würzburg, Germany

Reprint requests to Dr. M. K.; Fax: + 49 441 798 3326; E-mail: knipper@uni-oldenburg.de

Z. Naturforsch. **62a,** 490 – 494 (2007); received April 24, 2007

Impedance spectroscopy is used for studying the electrical transport properties of bulk heterojunction solar cells. A replacement circuit is needed to translate the frequency response of the circuit to the individual interfaces and layers of the solar cell. As a material combination and device architecture, composites of P3HT and PCBM, sandwiched between a transparent ITO front electrode and an aluminum back electrode, as well as a polymer buffer layer were investigated. By varying the film thickness we identified an equivalent circuit capable to fit our experimental data. We found a dielectric constant for the P3HT and for the P3HT:PCBM bulk.

Key words: Organic Solar Cells; Bulk Heterojunction; Impedance Spectroscopy; Equivalent Circuit.

1. Introduction

Conjugated polymers exhibit a high potential for the production of efficient and, at the same time, low-cost, flexible optoelectronic devices for large area applications [1]. Blended with suitable acceptors, it is possible to achieve efficient charge carrier generation [2]. Upon photoexcitation, an ultrafast electron transfer between the donor and the near acceptor takes place with a quantum efficiency close to unity [3, 4]. One popular material combination for polymer solar cells is the organic bulk heterojunction solar cell [5, 6]. Two different materials, namely the acceptor-type fullerene molecules and the p-polymer, form an interpenetrating network yielding a photoactive film with a large geometrical interface between donor and acceptor. Both materials are optically active and absorb light in a different frequency spectrum. The thin absorber film is sandwiched between two electrodes with asymmetric work functions. For solar cells based on the polymer-fullerene bulk heterojunction concept, a power conversion efficiency of 5% has been reported recently [7 – 10]. The material combination most frequently investigated in polymer photovoltaics is the p-type conjugated polymer poly [3-hexylthiophene-2,5-diyl] (P3HT) blended with the electron acceptor [6,6]-phenyl-C_{61} butyric acid methyl ester (PCBM).

By the help of impedance spectroscopy, we aimed at an analysis of the individual material components as well as the composites with and without a PEDOT:PSS interfacial layer. It allowed us to have a closer look at the internal device structure, the behaviour of the interfacial layer and the metal/P3HT junction. In a first step, we discuss an equivalent circuit diagram characterizing the P3HT absorber of the polymer-fullerene bulk heterojunction solar cell.

2. Experimental

ITO substrates were cleaned in an ultrasonic bath using acetone and isopropanol. After oxygen plasma etching, a PEDOT:PSS film was spin-coated onto the substrate and put on a hot plate at 150 °C for 15 min. The thickness of the PEDOT:PSS film varied from 75 nm to 220 nm. The next preparation steps and also the measurements were done in a glove box under nitrogen atmosphere. First, the polymer and the polymer-fullerene blend, respectively, was spin-coated and, after that, the metal (Al or Au) electrode (thickness 100 nm) was evaporated. The samples were contacted with gold fingers in order to perform electric spectroscopy measurements via a Solartron

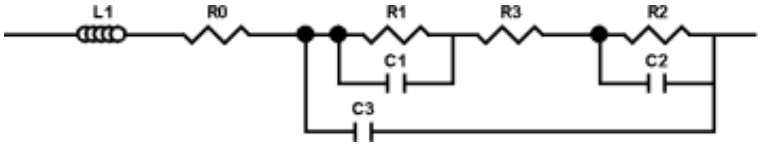

Fig. 1. Equivalent circuit for our devices. R_2 and C_2 correspond to PEDOT:PSS, R_3 and C_3 to P3HT, R_1 and C_1 are assigned to the P3HT / Al interface.

SI1260 impedance/gain phase analyzer. The measurements were done at 0 V DC bias in the dark. The voltage modulation was 30 mV and the frequency was swept from 0.05 Hz to $5 \cdot 10^6$ Hz, capturing the appropriate resistance and capacitance of the sample. With these values we calculated the complex resistance

$$Z = \frac{R}{1 + 2\pi \mathrm{i} RCf},$$

where R denotes the measured resistance, C the capacitance, and f the frequency. The real part, plotted over the imaginary part of the complex resistance, gives the Cole-Cole plot, also known as Nyquist plot.

3. Results

By varying the PEDOT:PSS and the active layer thickness, we found the equivalent circuit sketched in Figure 1. The inductance (L_1) is related to the connecting wires and becomes only dominant for frequencies above 1 MHz. It is connected in series. The feed lines and, especially, the ITO contact contribute to the serial resistance (R_0). To fit our experimental results, we need three RC networks in the equivalent circuit, where one capacitance (C_3) is parallel to the rest of the serial network, containing R_1 parallel to C_1, R_2 parallel to C_2, and R_3 (see Fig. 1).

Other equivalent circuits described in [11 – 13], containing two or three RC circuits connected in series [normally applied for, e. g., poly-phenylene-vinylene (PPV) devices] could not properly fit the thickness dependence of our experimental data. Though it was possible for these models to give a decent fit for one device with a fixed film thickness, upon variation of the individual layer thickness we had to vary the values of two or more capacitors to properly describe the transient response. From the device and circuit point of view, such an observation immediately suggests that the underlying model is physically incorrect. Further confirmation to disregard these replacement circuits came from the observation that we could not derive a well-defined dielectric constant for our materials.

Starting with a simple device structure (ITO / P3HT / Al) and assuming a parallel plate capacitor architecture ($C = \varepsilon_\mathrm{r}\varepsilon_0 A/d$, where A is the area, d the thickness, ε_r and ε_0 are the relative and absolute dielectric constant, respectively) with differently thick dielectrica, we could determine ε_r of P3HT to be around 3. This value was consistently found for a P3HT layer thickness from 45 nm to 360 nm. Next, PEDOT:PSS was introduced into the layer stack (ITO / PEDOT:PSS / P3HT / Al), and the replacement circuit was expanded by another RC element (C_2/R_2). Again, the thickness variation of the individual films allowed to undoubtedly assign the capacity C_3 to the P3HT layer. As already indicated above, the replacement circuit depicted in Fig. 1 gives an excellent fit for these stacks (see also Fig. 2) and allowed to determine the dielectric constant of P3HT with $\varepsilon_{\mathrm{r,P3HT}} = 3$, assuming a parallel-plate capacitor. Table 1 lists the dielectric constant for different film thicknesses of the P3HT layer, and the values are within less than 5% deviation. All simpler replacement circuits with one or more RC in series (up to three), did not properly describe the correlation between the layer thickness and the individual capacitances. Figure 2 compares the experimental data with the corresponding fit for one typical measurement. Figure 2a shows the imaginary resistance over the real resistance (Cole-Cole plot). In Fig. 2b, one can see the absolute value of the resistance versus the applied frequency and Fig. 2c plots the angle between the real and imaginary resistance versus the frequency. The quality of the fit to the experimental data was outstanding high.

Table 1. Fit results C_3 for a given device area A and changing thickness d; ε_r is calculated. Device structure: ITO / PEDOT:PSS / P3HT / Al. From the fit with the found equivalent circuit we got the capacitance C_3. The samples have a different active area A, and varying the P3HT film thickness d from 45 nm to 360 nm gives a dielectric constant of 3.

C_3 [nF]	A [mm^2]	d [nm]	ε_r (calculated)
0.59	8.2	360	2.9
0.63	8.6	340	2.8
0.59	4.9	230	3.1
1.25	6.8	150	3.1
2.69	5.9	60	3.1
3.84	6.4	45	3

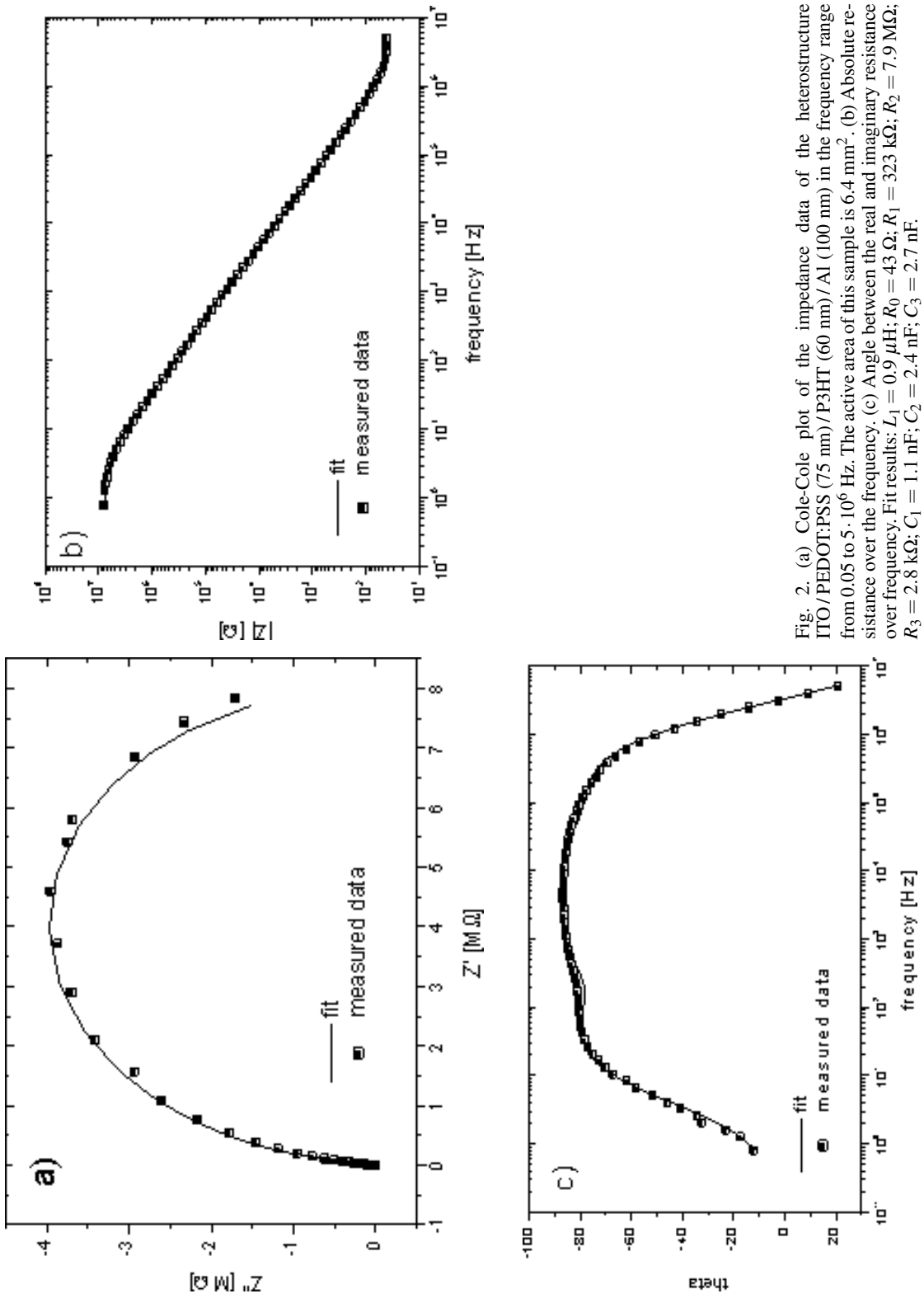

Fig. 2. (a) Cole-Cole plot of the impedance data of the heterostructure ITO / PEDOT:PSS (75 nm) / P3HT (60 nm) / Al (100 nm) in the frequency range from 0.05 to $5 \cdot 10^6$ Hz. The active area of this sample is 6.4 mm^2. (b) Absolute resistance over the frequency. (c) Angle between the real and imaginary resistance over frequency. Fit results: $L_1 = 0.9\ \mu$H; $R_0 = 43\ \Omega$; $R_1 = 323\ \text{k}\Omega$; $R_2 = 7.9\ \text{M}\Omega$; $R_3 = 2.8\ \text{k}\Omega$; $C_1 = 1.1$ nF; $C_2 = 2.4$ nF; $C_3 = 2.7$ nF.

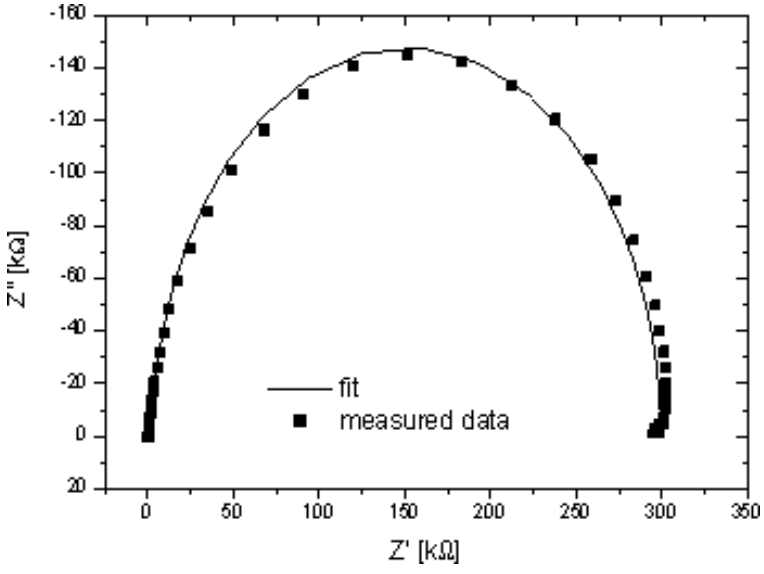

Fig. 3. Cole-Cole plot of the impedance data of the heterostructure ITO / PEDOT:PSS (125 nm) / P3HT:PCBM (120 nm) / Al (100 nm) in the frequency range from 0.05 to $5 \cdot 10^6$ Hz. The active area of this sample is 5.9 mm^2. Fit results: $L_1 = 0.8$ μH; $R_0 = 31$ Ω; $R_1 = 286$ kΩ; $R_2 = 11.9$ kΩ; $R_3 = 1.6$ kΩ; $C_1 = 2.1$ nF; $C_2 = 2.0$ nF; $C_3 = 1.8$ nF.

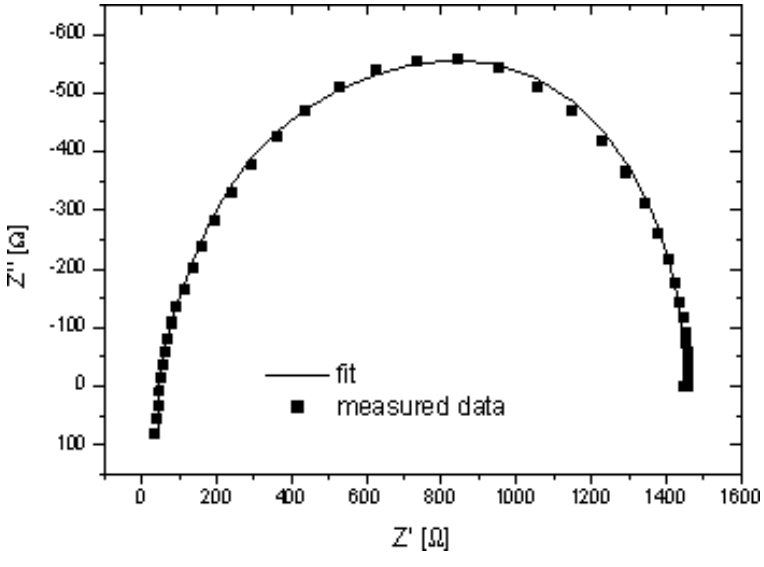

Fig. 4. Cole-Cole plot of the impedance data of the heterostructure ITO / PEDOT:PSS (75 nm) / P3HT:PCBM (120 nm) / Au (100 nm) in the frequency range from 0.05 to $5 \cdot 10^6$ Hz. The active area of this sample is 5.3 mm^2. Fit results: $L_1 = 3.5$ μH; $R_0 = 40$ Ω; $R_1 = 485$ Ω; $R_2 = 553$ Ω; $R_3 = 373$ Ω; $C_1 = 1.8$ nF; $C_2 = 9.7$ nF; $C_3 = 1.3$ nF.

So far we have been able to establish a correlation between the replacement circuit elements 2 and 3 to the PEDOT:PSS and to the semiconductor layer, respectively. Before analyzing the origin of the remaining RC element 1 (R_1/C_1), we will discuss the impedance of a fully working solar cell, where the P3HT layer has been replaced by a P3HT / PCBM composite.

Figure 3 summarizes the findings for ITO / PEDOT:PSS / P3HT:PCBM / Al devices. Again, a variation of the film thickness of the individual layers has been performed to control the validity of the replacement circuit, and a satisfying correlation was found by attributing R_2C_2 and R_3C_3 to the PEDOT:PSS layer and to the semiconductor layer, respectively. Interestingly, it was necessary to adapt the dielectric constant for the P3HT / PCBM to a slightly higher value ($\varepsilon_{r,P3HT/PCBM} = 3.3$) as compared to pristine P3HT ($\varepsilon_{r,P3HT} = 3$). Figure 3 shows a typical measurement for this device architecture.

From all the investigations so far, the remaining element capacitance could not be attributed to a physical layer. The assumption to assign this capacitance to an interface instead is therefore reasonable. An educated guess is, that this capacitance origins from a de-

pletion layer at the P3HT:PCBM / Al interface in this device.

The ITO / PEDOT interface can be excluded, since C_1 was also observed for ITO / P3HT / Al devices. To verify this assumption, we have changed the metal electrode from aluminum to gold. A significant reduction of the resistance R_1 by more than 3 orders in magnitude was observed (compare Figs. 3 and 4) while C_1 remained unchanged, confirming the assumption that R_1/C_1 origins from the metal / semiconductor interface. The depletion regions turned out to be relatively thin in the case of a gold contact (~ 5 nm), and increased up to 20 nm in case of an aluminium contact. In parallel, the active layer thickness reduced by the strength of the depletion layer. Under these assumptions, we have been able to get an excellent fit quality for both types of contacts with the same set of parameters for the individual layers (see Fig. 4).

4. Conclusion

We have presented a consistent replacement circuit for polymer-fullerene solar cells from impedance spectroscopy. With this model we were able to fit all our experimental data with one set of parameters. A thickness variation of the individual layers allowed to identify the replacement circuit elements for PEDOT:PSS as well as for the semiconductor layers P3HT and P3HT:PCBM. The variation of the top electrode from aluminum to gold clarified the origin of the third element (C_1/R_1). It is due to a depletion layer between the semiconductor and the metal electrode.

Having established this, the replacement circuit opens up many opportunities to more precisely investigate and better understand polymer devices. One of the immediate benefits of the replacement circuit is gained in degradation and reliability studies, allowing to uniquely distinguish between interfacial or contact degradation versus bulk or material degradation.

Acknowledgement

Financial support from the German Federal Ministry for Education and Research (BMBF) under Contract No. 03N2023A-E (EKOS) is gratefully acknowledged.

[1] H. S. Nalwa (Ed.), Handbook of Organic Conductive Molecules and Polymers, Vols. 1 – 4, Wiley, New York 1997.
[2] P. Schilinsky, C. Waldauf, and C. J. Brabec, Appl. Phys. Lett. **81**, 3885 (2002).
[3] N. S. Sariciftci, L. Smilowitz, A. J. Heeger, and F. Wudl, Science **258**, 1474 (1992).
[4] C. J. Brabec, G. Zerza, G. Cerullo, S. De Silvestri, S. Luzatti, J. C. Hummelen, and N. S. Sariciftci, Chem. Phys. Lett. **340**, 232 (2001).
[5] G. Yu, J. Gao, J. C. Hummelen, F. Wudl, and A. J. Heeger, Science **270**, 1789 (1995).
[6] C. J. Brabec, V. Dyakonov, J. Parisi, and N. S. Sariciftci (Eds.), Organic Photovoltaics – Concepts and Realization, Springer, Berlin 2003.
[7] J. Xue, B. P. Rand, S. Uchida, and S. R. Forrest, J. Appl. Phys. **98**, 124903 (2005).
[8] W. Ma, C. Yang, X. Gong, K. Lee, and A. J. Heeger, Adv. Funct. Mater. **15**, 1617 (2005).
[9] G. Li, V. Shrotriya, J. Huang, Y. Yao, T. Moriarty, K. Emery, and Y. Yang, Nat. Mater. **4**, 864 (2005).
[10] L. L. Kazmerski, J. Electron. Spectrosc. Relat. Phenom. **150**, 105 (2006).
[11] M. Meier, S. Karg, and W. Riess, J. Appl. Phys. **82**, 1961 (1997).
[12] M. Esteghamatian and G. Xu, Synth. Met. **75**, 149 (1995).
[13] H. C. H. Martens, W. F. Pasveer, H. B. Brom, J. N. Huibert, and P. W. M. Blom, Phys. Rev. B **63**, 125328 (2001).